chemosensors

MDPI

Article

Rapid Matching Antibodies Pair and Fast Detecting Melioidosis with Fluorescent Immunochromatographic Test Strips

Yi-Zhi Lin [1], Ting-Ting Zhou [2], Jin Zhu [2] and Shou-Nian Ding [1,*]

[1] Jiangsu Province Hi-Tech Key Laboratory for Bio-Medical Research, School of Chemistry and Chemical Engineering, Southeast University, Nanjing 211189, China; lin_yizhi@seu.edu.cn
[2] Huadong Medical Institute of Biotechniques, Nanjing 210002, China; ahzt128@126.com (T.-T.Z.); zhujin1968@njmu.edu.cn (J.Z.)
* Correspondence: snding@seu.edu.cn; Fax: +86-25-52090621

Abstract: The high infectivity, difficulty to diagnose, and high drug resistance of melioidosis limited the timeliness of treatment. Lateral flow assay (LFA) was operated in this research to provide an instant diagnosis method, and a fast antibody rapid matching test strategy based on LFA was developed to select the most sensitive and specific pair of antibodies. Compared to the traditional ELISA method, the new matching strategy limits the pairing time to 3 h without any complex instruments. The rapid pairing test strategy is a universal strategy that is suitable for various sandwich immune antigen pairings. To fasten the test of the test strips, dry fluorescence immunoassay analyzer (DFIA) was designed and applied. The equipment also simplifies the process of data acquisition. Finally, the concentration gradient test was operated, and the detection lines and limits were presented.

Keywords: melioidosis; antibody matching; carbon dots; fluorescence

Citation: Lin, Y.-Z.; Zhou, T.-T.; Zhu, J.; Ding, S.-N. Rapid Matching Antibodies Pair and Fast Detecting Melioidosis with Fluorescent Immunochromatographic Test Strips. *Chemosensors* **2023**, *11*, 351. https://doi.org/10.3390/chemosensors11060351

Academic Editor: Jin-Ming Lin

Received: 25 May 2023
Revised: 13 June 2023
Accepted: 18 June 2023
Published: 19 June 2023

1. Introduction

Melioidosis is a zoonosis disease caused by *Burkholderia pseudomallei* (Bacillus Melioides) which belongs to facultative intracellular Gram-negative bacterium [1]. About 89,000 people are killed by this disease annually [2]. People and animals can be infected by skin abrasion, inhalation, or ingestion [3]. It is highly infectious, difficult to diagnose, and highly drug resistant, and there is no corresponding vaccine [4]. It has been listed as a Class B bioterrorism agent by WHO. As reported, hemolysin coregulated protein 1 is the virulence factor of melioidosis which can stimulate the body to produce specific antibodies. It has potential application value in serological identification, screening of vaccine candidate antigens, and lateral flow assay.

Several assays have been developed to diagnose melioidosis aside from bacteria culture. PCR has been developed but is not in routine practice because of its low sensitivity which most likely stemmed from the low concentration of *Burkholderia pseudomallei* in blood and the co-purification of PCR inhibitors with target DNA [5]. The indirect hemagglutination assay (IHA) is a rapid and cheap method [6] used to detect antibodies produced by human beings during infection that are specific to *Burkholderia pseudomallei* [7,8]. However, the test is unreliable because in areas where *Burkholderia pseudomallei* are widely prevalent, most people have the target antibodies in their blood, which results in a false-positive test result but no infection. This drawback makes this detection method completely unsuitable for detecting viruses and bacteria that have been around in an area for a long time, such as melioidosis. Antigen detection by immunofluorescence assay (IFA) is highly sensitive and specific [9]. However, this assay requires a fluorescent microscope and a medical practitioner with requisite expertise that will not be available in most endemic settings. This method can only be applied to epidemiological investigations before an outbreak, and its application is limited to some extent.

Lateral flow assay (LFA) is a technique for producing two or more bands by the specific combination of substances in the sample through the liquid flow generated by dropping the liquid sample with the prefabricated test strip containing dry reagent, so as to obtain the test results [10]. It has been widely applied in the test of pregnancy, failure of internal organs, and virus or bacteria such as COVID-19 causing the global pandemic [11,12]. LFA has been highly valued because of its low price, fast speed, and ease of use [13]. However, its sensitivity has been questioned and compared with other analysis reference methods [14]. The most commercially applied label is Au NPs for its excellent stability, incomparable biocompatibility, simpler synthesis, and distinguishable visual effect. To enhance LFA strips' sensitivity, researchers utilized magnetic materials or field [15,16], carbon materials [17,18], fluorescent quantum dots (QDs) [19–21], upconversion phosphor [22], and organic fluorescent dye [23] as labels to structure LFA test strips. In all reinforcement strategies, integrating fluorescent quantum dots into nanospheres is one of the most efficient methods because the fluorescence intensity of a fluorescent nanosphere is much higher than that of single QD. At the same time, compared to traditional semiconductor QDs, a fluorescent nanosphere has the advantage of high biocompatibility, high stability in complex solution, and convenient operation [24].

Another widely operated signaling material is latex for its multiple colors and excellent stability. The advantage of latex endows it with the ability to detect multiple components simultaneously [25]. For instance, Chen et al. combined red, green, and blue latex microspheres in LFA to detect aflatoxin B1, T-2 toxins, and zearalenone in cereals simultaneously [26]. Magnetite nanoparticles, which are normally colloidal iron oxide (Fe_3O_4), are a yellow or black signaling material by naked eyes or a magnetic signal provider with external equipment [27–29]. The detection time of magnetite nanoparticles is related to the size, and the signal strength is closely related to the magnetite concentration. This capability provides another signal for LFA, which also has a much higher accuracy than traditional Au NPs. Furthermore, phosphorescence is a slow-emitting and light-cooling luminescence phenomenon [22,30]. When the phosphorescent material is irradiated by incident light of a specific wavelength, it enters the excited state and emits phosphorescence. He et al. used the highly erbium-doped and the thulium ions-doped upconversion nanoparticles to achieve the highly sensitive detection of prostate-specific antigen and ephrin type-A receptor 2. Additionally, a common chemiluminescent lateral flow assay (CLLFA) is used to label the antibody with horseradish peroxidase (HRP) [31–33]. After the common steps of LFA, luminol, chemiluminescent enhancer, and hydrogen peroxide (H_2O_2) are added to the CLLFA, the test line will achieve a blue glow. The reagents to be stored and mixed prior to the measurement increase the cost and decrease the user-friendliness. Photothermal nanomaterials are also promising LFA-labeled probes. The thermal detection-based platforms offer many advantages over the colorimetric LFA for its high photothermal conversion efficiency with a low background signal. However, it still needs a laser source to emit which cannot be reached easily.

As members of quantum dots, carbon dots are a class of novel zero-dimensional nanomaterials in the carbon family. Compared to traditional semiconductor QDs, fluorescent carbon dots (CDs) have advantages in chemical inertness, photostability, low cytotoxicity, and biocompatibility [34,35]. As a result, CDs have several applications in biological imaging [36], drug delivery [37], sensor technology [38], photocatalysis [39], and other fields. Several mechanizations, including surface state, carbon core state, molecule state, and synergistic effect, are involved in the luminescence of CDs [40]. Fortunately, even though the mechanization of CDs is not immediately apparent, the variety of raw materials offers sufficient opportunity for the creation of CDs with extremely high quantum yield (QY). All kinds of carbonaceous raw material contain the capability to form carbon point. During the formation of CDs fluorescent spheres, silane coupling agents act as coordination solvent to synthesize or modify CDs, thereby grafting and passivating CDs. This can effectively prevent the accumulation of CDs and make the fluorescent sphere containing CDs have solid fluorescence. CDs have a small size (<10 nm) and contain abundant func-

tional groups on the surface. To avoid the difficulties of purification/extraction of CDs and surface modification of CDs during formation of CDs fluorescent spheres, the in situ synthesis of CDs inside the pre-synthesized silica spheres is an excellent strategy and can simplify the synthesis of CDs fluorescent spheres.

A diagnostic LFA for melioidosis has been developed, which is named Active Melioidosis Detect (AMD) [41]. The assay targets the *Burkholderia pseudomallei* capsular polysaccharide (CPS) using a CPS-specific monoclonal antibody. Compared to previous described methods, AMD is a convenient and fast detection method. Many researchers focus on the development of AMD, so that its reliability continues to improve. The major benefit is that AMD enables its test results to be obtained in less than an hour after the clinical sample being collected. Although the sensitivity of AMD is lower than culture results, the gold standard for diagnosis of melioidosis, the culture results are rarely available within 24 h or take even several days. The sensitivity of AMD is still enough that a positive result enables the clinician to institute therapy targeting *Burkholderia pseudomallei* and to operate further additional cultures and imaging to make a definite diagnosis.

Due to the complexity of protein structure, there may be non-specific binding sites between antibodies of the same antigen. This leads to non-specific adsorption between antibodies. At the same time, the binding ability of different antibodies to the same antigen is also strong or weak. Therefore, for sandwich immunobiological detection methods, antibody screening and pairing are extremely necessary. To match antibody pairs in all kinds of LFA research, the ELISA method is widely used by all researchers [42]. ELISA is also named an enzyme-linked immunosorbent assay, which is currently the most widely used immunoenzyme technology for qualitative or quantitative detection of antibodies or antigens. The ELISA test is a sensitive and specific method, but the requirement of devices limits its convenience in all laboratories in universities and hospitals when it is applied in antibodies matching. The increased testing time has increased the necessity of preserving freshly purified antibodies and increased the requirements for antibody preservation. At the same time, the materials prepared during the pairing process cannot be applied to subsequent LFA research, resulting in a large amount of antibody waste, as well as increased material and time costs for research, which undoubtedly lead to delays in research progress.

This article shows that CDs-based silica spheres (CSS) can be synthesized by growing CDs in situ inside the (aminoethyl)-γ-aminopropyltrimethoxysilane (AEAPTMS)-grafted silica nanospheres by a one-step hydrothermal method. The CSS is chosen by its high QY (near 90%) and excellent dispersion, solubility, and stability in aqueous solution. Its bright blue fluorescence enhances the sensitivity of Hemolysin-Coregulated Protein 1 (Hcp-1) of melioidosis and helps us develop the CSS-LFA technology for melioidosis. To select an appropriate pairing of antibodies, a rapid pairing test strategy is applied. Compared to the traditional ELISA method, it only takes about 3 h to elect the appropriate pairing. A new type of equipment called dry fluorescence immunoassay analyzer (DFIA) was developed and applied to detect blue fluorescent LFA test strips. The equipment speeds up the test and simplifies the process of data acquisition. With the application of ImageJ and DFIA, the test lines and detection limits were obtained in the end.

2. Materials and Methods

2.1. Reagents

Triethanolamine, cetyltrimethyl ammonium bromide (CTAB), sodium salicylate, tetraethyl silicate (TEOS), ethanol, concentrated hydrochloric acid (HCl), ammonia, (aminoethyl)-γ-aminopropyltrimethoxysilane (AEAPTMS), 3-aminopropyltriethoxysilane (APTES), citric acid, sodium citrate, saccharose, Polyvinylpyrrolidone (PVP) 55 K, anhydrous ethanol, and DMF were purchased from Sinopharm Group Chemical Reagent Co., Ltd., Shanghai, China. EDC was purchased from Shanghai Titan Scientific Co., Ltd., Shanghai, China. BSA was purchased from Autogyro Biotechnology Co., Ltd., Shanghai, China. Hcp-1 antigen and its antibodies consist by Jiangsu Provincial Center for Disease

Control and Prevention, China and control and prevention were also provided by them. Normal serum was obtained from Jiangsu First People's Hospital, Nanjing, China. Hcp antibodies and antigen were received from Huadong Medical Institute of Biotechniques, Nanjing, China. Goat Anti-mouse Immunoglobulin G (IgG), Sample Pad, NC Film, Absorbent Pad, and Polyvinyl chloride (PVC) Substrate were purchased from Shanghai Jieyi Biotechnology Co., Ltd., Shanghai, China.

2.2. Fabrication of the CSS-Based LFA Test Strip

The sample pad was divided into strips measuring 12 mm in length, dipped into a PBS solution (pH 7.4, 0.01 M) containing 2% NaCl (*w*/*v*), 0.1% Tween-20 (*v*/*v*), 1% saccharose (*w*/*v*) and 1% polyvinylpyrrolidone 55 K (*w*/*v*), and then removed to dry and set aside. The test (T) line was created by uniformly distributing 2 mg/mL of coated capture Hcp-1 antibody on the NC membrane, while the control (C) line was created by evenly distributing 2 mg/mL of diluted IgG on the NC membrane. It was then dried for subsequent use in a 37 °C oven for two hours. The PVC substrate, NC membrane, pretreatment sample pad, and absorbent pad were then put together. The sample pad and the absorbent pad were then adhered to the ends of the PVC substrate, respectively, after the NC membrane had been pasted in the center. There is a 1–2 mm overlap between the NC membrane, sample pad, and absorbent pad, respectively. The completed PVC substrate was sliced into 3 mm wide strips by the cutting machine, which then stored them at 4 °C for subsequent use.

2.3. Expression and Purification of Hemolysin-Coregulated Protein 1

The DNA sequence from *Burkholderia pseudomallei* BPC006 encoding Hcp-1 was cloned into pET-28a with an N-terminal His6-tag. Production of Hcp-1 protein was induced in BL21 (DE3) cells (Novagen, Darmstadt, Germany) by addition of 0.1 mM isopropyl-b-D-thiogalactoside (IPTG) at 37 °C in LB broth. Bacterial cells were harvested at 6 h post induction at 25 °C by centrifugation at 6000 g for 10 min, and His-tagged protein was purified by HisTrapTM affinity column (GE Healthcare, Chicago, IL, USA). All elution fractions were collected and detected by SDS-PAGE. The Hcp-1 protein was concentrated with 10 kDa MWCO (Millipore Corporation, Billerica, MA, USA). The proteins were dialyzed extensively against PBS and stored at −80 °C.

2.4. Development of Anti-Hcp-1 mAb

The anti-Hcp-1 mAb was generated as previously described [43]. Briefly, BALB/c mice (SLAC Laboratory Animal Company, Shanghai, China) were subcutaneously injected with 50 μg purified Hcp-1 protein and Freund's complete adjuvant. Spleen cells were fused with SP2/0 by PEG to develop hybridomas cells in HAT selective medium (Gibco, Billings, MT, USA). Positive hybridoma cells selected by ELISA were intraperitoneally injected into BALB/c mice, and ascites were collected after 7 days. Anti-Hcp-1 mAb was purified by using our previously published protocol and confirmed by WB [43].

2.5. Synthesis of Dendritic SiO_2 Spheres

Dendritic SiO_2 was synthesized by traditional Stöber method. TEA (68 mg) was added into H_2O (25 mg) and stirred at 80 °C for 30 min. Then, CTAB (380 mg) and sodium salicylate (168 mg) were added into the solution and stirred for 1 h. TEOS (4 mg) was injected into the solution and the mixture was stirred gently at 80 °C for 2 h. The mixture was then diluted with ethanol and sedimentation was separated by centrifugation. The precipitates were washed with ethanol for several times and finally dispersed in HCl/ethanol mixture and stirred at 60° C for 24 h to extract the residue organic templates. The dendritic SiO_2 spheres ($dSiO_2$) were washed with ethanol and H_2O and finally dispersed in ethanol.

2.6. In Situ Synthesis of CDs Dendritic SiO_2 Spheres (CSS)

The synthesis strategy was learned from Xu L.D [21]. AEAPTMS (360 μL) was added into ethanol (100 mL) which disperses $dSiO_2$ nanospheres (100 mg). When the dispersion

was uniform, ammonia (2 mL) was added into the mixture and stirred for 12 h. After that, the precipitate was separated by centrifugation and purified to obtain AEAPTMS-grafted $dSiO_2$ nanospheres. To practice in situ synthesis of CDs into foresaid nanospheres, 2 mL of aqueous solution containing sodium citrate (0.0037 g) was added into 7 mL DMF dispersing AEAPTMS-grafted $dSiO_2$ nanospheres (10 mg). After the mixture was uniform, it was reacted in an oven at 220 °C for 30 min in the inner pot of the autoclave. After cooled to natural temperature, CSS synthesized in the reaction was washed to obtain CSS.

2.7. Preparation of CSS-Labeled Antibody Conjugate

APTES (20 μL) and ammonia (5 mL) were added into ethanol (5 mL) dispersing CSS (5 mg). After stirring for 6 h, it was washed and separated and dispersed in 5 mL of DMF, and then succinic anhydride (50 mg) was added. After stirring for 6 h, washing was performed to obtain carboxy-terminated CSS. Subsequently, 0.5 mL of aqueous solution containing 1 mg of CSS, 20 μL of EDC aqueous solution (10 mg/mL), and 0.5 mL of PBS (pH 7.4, 0.01 M) buffer containing 80 μg of labeled antigen against Hcp-1 were sequentially mixed. After shaking at room temperature for 2 h, the solution was centrifuged under 10,000 RPM for 3 min and the product was dispersed in 1 mL of PBS (pH 7.4, 0.01 M) buffer containing 1% BSA (*w*/*v*) to prepare CSS-labeled antibody conjugate.

2.8. Detection of Hcp-1 with CSS-Based LFA Test Strips

CSS-labeled antibody PBS (0.01 M) solution was mixed with Hcp-1 recombinant protein solutions of different concentrations. The uniformed mixed solution was then dropped on the pretreated sample pads of the test strips. After a waiting period of about 25 min, the result can be observed under 365 nm UV lamp. The picture for further research was taken by Huawei mobile phone. The test strips are then fixed into a standard test card for the application of dry fluorescence immunoquantitative analyzer (DFIA).

3. Results and Discussion

The in situ growth of CDs in dendritic SiO_2 spheres is an easy method of synthesis of carbon quantum dots. Transmission electron microscopy (TEM) characterization was used to analyze the dendritic SiO_2 spheres ($dSiO_2$) and the CDs inside the groove of the spheres. As shown in Figure 1b, the size of $dSiO_2$ is around 180 nm and the microsphere contains an enormous superficial area to accommodate the CDs to aggregation of luminescent clusters inducing the enhancement of fluorescence, as shown in Figure 1a,c. The synthesis is a one-step method under solvothermal conditions in the presence of AEAPTMS. The carbon dots grow inside the dendritic SiO_2 spheres because AEAPTMS provides anchor points for raw materials on dendritic silica. The amino group combines with the carboxyl group in the reaction material in solution, thereby enabling the connection of the core of carbon dots to the dendritic SiO_2 spheres. However, the combination method limits the type of raw materials. As shown in Figure 2a, the 3D fluorescence plots of CSS show that the emission peak is 455 nm under the excitation wavelength of 354 nm. The fluorescence emission spectrum under 354 nm excitation light is shown in Figure 2b. Under the common 365 nm excitation light source, its maximum emission intensity is still 93.7% of the aforementioned maximum emission intensity with similar emission wavelengths of 460 nm. The quantum yield (QY) of CSS aqueous solutions is 89.3%, respectively. The method for measuring fluorescence quantum yield is the reference method, which uses the fluorescence signal of the reference substance to compare the fluorescence signal of the measured substance and calculate the fluorescence quantum yield of the measured substance. In the experiment, we used quinine sulfate solution (QY = 54% under 360 nm excitation light) as a reference fluorescence standard. The equation is Φu = ΦsFuAs/FsAu (Φu and Φs means fluorescence quantum yield of the substance to be tested and the reference substance; Fu and Fs means integrated fluorescence intensity of the substance to be tested and the reference substance; Au and As means the absorbance of the substance to be tested and the reference substance).

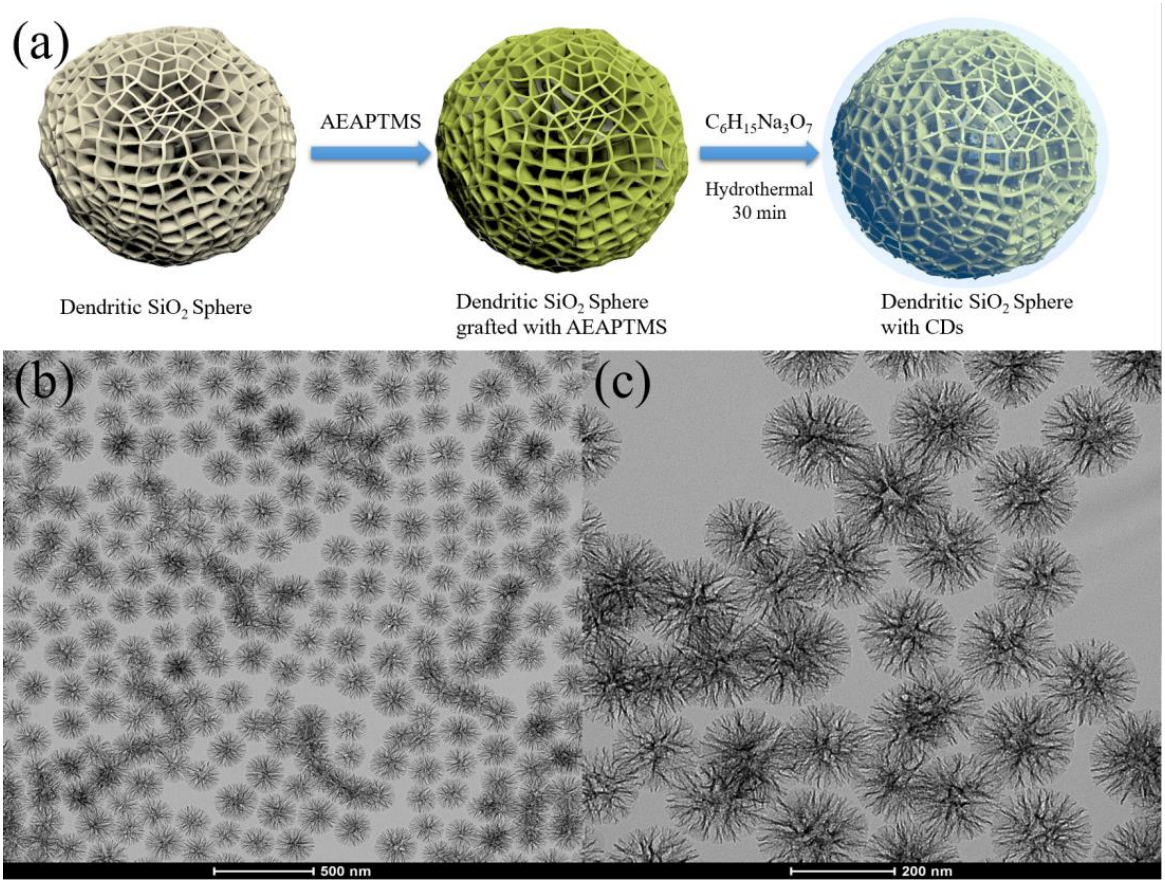

Figure 1. (**a**) Synthesis of high QY in situ growth nanospheres; (**b**) TEM images of dendritic SiO_2 spheres; (**c**) Dendritic SiO_2 spheres with in situ growth CDs (CSS).

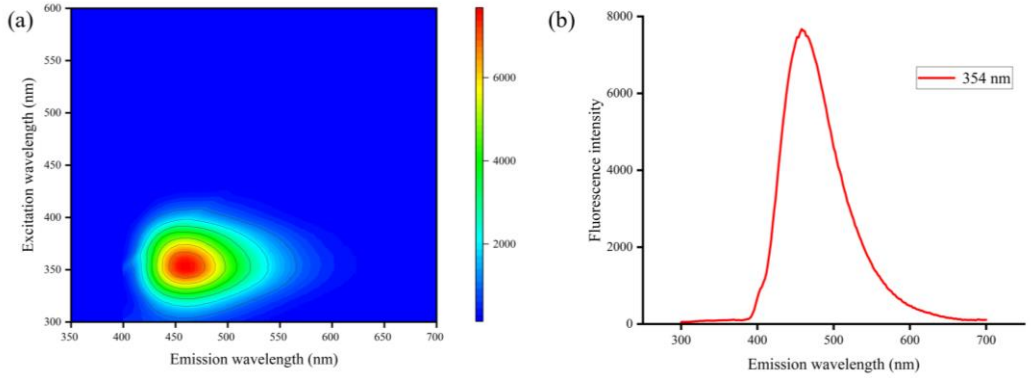

Figure 2. (**a**) 3D fluorescence plots of CSS; (**b**) best fluorescence emission spectrum under 354 nm.

For the well binding and fluorescence properties, we designed a rapid antibody matching test strategy in about 3 h. In this experiment, four different antibodies of Hcp-1, named 1A201, 2D113, 2B101, and 3B1, were matched with this strategy. To pick out the minimum non-specific adsorption and most sensitive pair of antibodies, four different CSS-antibody conjugate and four different LFA test strips with four different test lines with antibodies above were prepared as shown in Figure 3a and zeta potential proved they were successfully synthesized as shown in Figure 3b. In Figure 3a, the Hcp-1 Ab1, named the detection antibody, was fixed on the CSS to combine with the antigens (Ag) in the sample. The Hcp-1 Ab2, named the capture antibody, applies to the surface of the NC membrane to capture Ab1-Ag conjugates in the liquid. This method is called sandwich immunity. After that, a cross-pair experiment was operated, in which 12 pairs of different

antibodies matching tests and corresponding blank control strips were applied to the test as shown in Figure 4a. The pair of 1A201 as detection antibody and 2D113 or 2B101 as capture antibody are shown in Figure 4a. From the analysis by ImageJ, we select 2D113 as capture antibody to perform further research for its higher T/C. Other pairs exhibit varying degrees of non-specific adsorption which makes the limit of detection be much higher than the pairs of no non-specific adsorption. At the same time, the brightness of the line is lower compared to the chosen pair. By applying this matching strategy, the matching time can be limited to 3 h, which rapidly diminishes the time of matching antibody pairs and provides a good foundation for large-scale screening of sandwich immune antibody pairs. The CSS-antibody conjugate and prepared test strips can immediately apply to subsequent concentration gradient testing to cut down the use of valuable and precious antibodies and save a significant amount of time for preparing experimental materials.

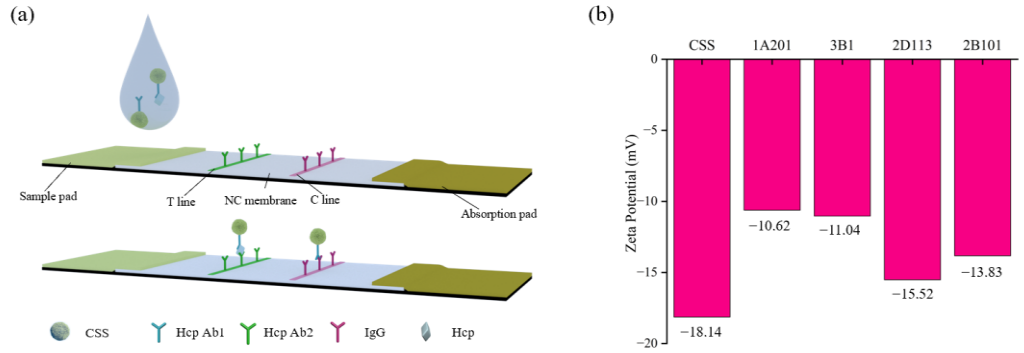

Figure 3. (**a**) LFA test strips and test method; (**b**) zeta potential of CSS and CSS conjugates.

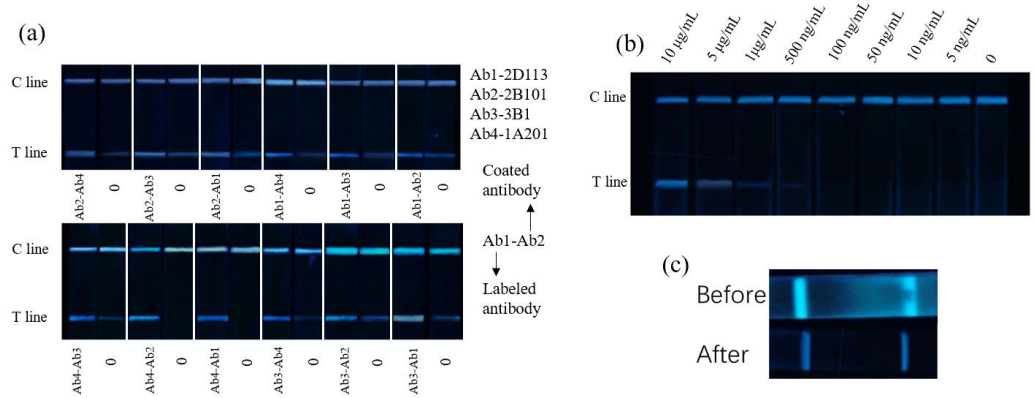

Figure 4. (**a**) Pairs of different matches in fast antibody rapid matching test strategy; (**b**) concentration gradient test; (**c**) comparison of sample pads before and after optimization.

At the same time, to eliminate background fluorescence, the sample pad was pre-processed. The comparison of them is similar to Figure 4c. The background fluorescence of the test strips was strongly affected by the composition of chromatographic solution. In order to add components other than antigen and marker conjugates, the pre-treatment sample pad is the most convenient method. When the sample solution to be tested is dripped onto the sample pad, the substance pre-treated on the sample pad will quickly dissolve in the test solution. This eliminates the step of adding these treatment solutions to the sample, thus simplifying the testing steps. From Figure 4c, it is obvious that the background fluorescence is eliminated to an acceptable level.

Applying the above pairing, the concentration gradient test was carried out. The initial test concentration gradient and the initial gradient is 10 μg/mL. As shown in Figure 4b, the naked eye detection limit is approximately 1 μg/mL. In past research, active melioidosis detect (AMD) LFA with colloidal gold nanoparticles was widely developed [44–47].

However, most of the research was focused on qualitative research in which sensitivity was reflected in positive accuracy rather than accurate concentration. The assay targets the *Burkholderia pseudomallei* capsular polysaccharide (CPS) using a CPS-specific monoclonal antibody. Compared to Hcp-1 of *Burkholderia pseudomallei*, its antigen specificity is lower, resulting in a lower positive reference value and susceptibility to interference from similar bacteria. With the processing of ImageJ, the test line is shown in Figure 5a and the accurate limit is down to 25.6 ng/mL. The application of the test line can help clinicians to determine and monitor the stage of the disease and increase the accuracy and effectiveness of treatment so as to reduce the side effects of treatment and help patients recover faster.

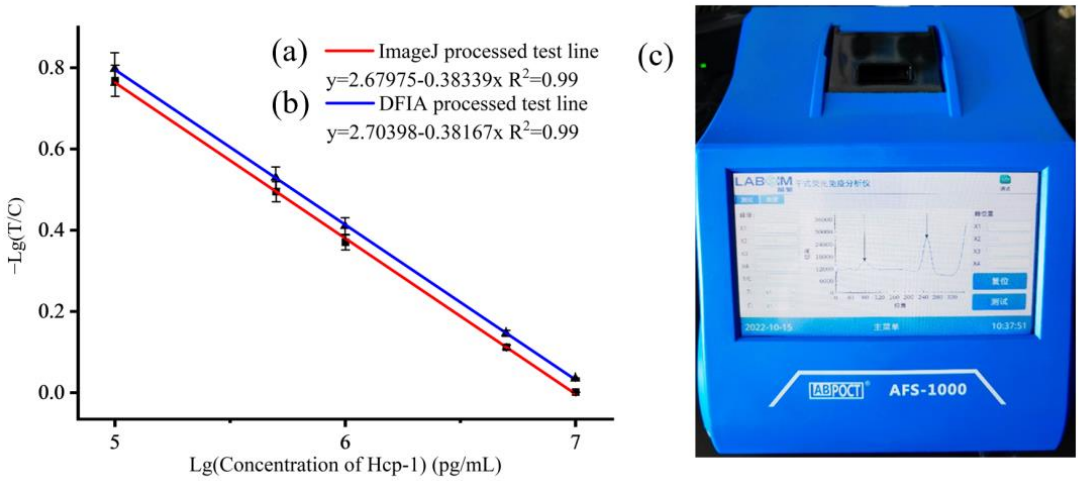

Figure 5. (**a**) Test line of Hcp-1 processed by ImageJ; (**b**) test line of Hcp-1 processed by DFIA; (**c**) dry fluorescence immunoassay analyzer (DFIA).

To increase the speed of interpretation of the LFA test strips, dry fluorescence immunoassay analyzer (DFIA) was developed and applied to detect blue fluorescent LFA test strips, as shown in Figure 5c. The analyzer is composed of an optical unit, mechanical unit, control unit, output display unit, and detection system component card. When the sample detection card is inserted into the dry fluorescence immunoquantitative analyzer, the processor controls the mechanical transmission device to transmit the detection card to the laser detection area. The excitation light (365 nm) source illuminates the detection card, and then the emission luminescence signal is collected and converted into an electrical signal. The control unit collects signals, calculates the content of analytes in the test samples automatically according to the software, and outputs them to the display screen or prints them out by its thermal printer. From the screen, the numerical value of fluorescence intensities including test line and control line and the value of T/C can be seen. In Figure 5a,b, it is obvious that the sensitivity of DFIA is lower than ImageJ (the accurate limit is about 41.1 ng/mL), but it is much easier to use.

4. Conclusions

In this article, to detect melioidosis, we structured a fast antibody rapid matching test method and selected a characteristic protein of melioidosis to operate an LFA fluorescent immunochromatographic test strips testing method. In the testing, an extremely high quantum yield in situ growth of CDs in dendritic SiO_2 spheres was applied as the fluorescent labels to offer a bright fluorescent signal for further analysis. Compared to the traditional antibody matching method, ELISA, our new method uses no expensive devices and saves time. In subsequent research of Hcp-1, the detection lines by ImageJ and dry fluorescence immunoassay analyzer are shown.

Author Contributions: Conceptualization, S.-N.D.; methodology, Y.-Z.L., T.-T.Z., J.Z. and S.-N.D.; validation, Y.-Z.L. and T.-T.Z.; investigation, Y.-Z.L.; resources, T.-T.Z.; data curation, Y.-Z.L. and

T.-T.Z.; writing—original draft preparation, Y.-Z.L. and T.-T.Z.; writing—review and editing, Y.-Z.L. and S.-N.D.; visualization, Y.-Z.L.; supervision, S.-N.D.; project administration, S.-N.D. and J.Z.; funding acquisition, S.-N.D. and J.Z. All authors have read and agreed to the published version of the manuscript.

Funding: This work was supported by the National Key Research and Development Program of China (2017YFA0700404), the National Science and Technology Major Project of China (AWS17J016, 2019SWAQ05-5-4), the National Natural Science Foundation of China (21535003, 21575022), and the Key Research and Development Plan of Jiangsu Province (BE2018617).

Institutional Review Board Statement: Not applicable.

Informed Consent Statement: Not applicable.

Data Availability Statement: The data presented in this study are available on request from the corresponding author. The data are not publicly available due to the requirement of collaborator (Huadong Medical Institute of Biotechniques) that all experimental data should not be disclosed.

Conflicts of Interest: The authors declare no conflict of interest.

References

1. Wiersinga, W.J.; Currie, B.J.; Peacock, S.J. Melioidosis. *N. Engl. J. Med.* **2012**, *367*, 1035–1044. [CrossRef]
2. Limmathurotsakul, D.; Golding, N.; Dance, D.A.B.; Messina, J.P.; Pigott, D.M.; Moyes, C.L.; Rolim, D.B.; Bertherat, E.; Day, N.P.J.; Peacock, S.J.; et al. Predicted global distribution of Burkholderia pseudomallei and burden of melioidosis. *Nat. Microbiol.* **2016**, *1*, 15008. [CrossRef]
3. Cheng, A.C.; Currie, B.J. Melioidosis: Epidemiology, pathophysiology, and management. *Clin. Microbiol. Rev.* **2005**, *18*, 383–416, Correction in *Clin. Microbiol. Rev.* **2007**, *20*, 533. [CrossRef]
4. Zhang, M.; Hu, Z.; Xia, Y.; Yuan, S.; Yan, J.; Rao, C.; Li, Q.; Yang, W.; Mao, X. Recombinant expression and immunological characterization of hemolysin coregulated protein 1,Burkholderia pseudomallei type VI secretion system protein. *J. Third Mil. Med. Univ.* **2020**, *42*, 2296–2301.
5. Richardson, L.J.; Kaestli, M.; Mayo, M.; Bowers, J.R.; Tuanyok, A.; Schupp, J.; Engelthaler, D.; Wagner, D.M.; Keim, P.S.; Currie, B.J. Towards a rapid molecular diagnostic for melioidosis: Comparison of DNA extraction methods from clinical specimens. *J. Microbiol. Methods* **2012**, *88*, 179–181. [CrossRef] [PubMed]
6. Gupta, R.K.; Sharma, S.B.; Ahuja, S.; Saxena, S.N. Indirect (Passive) hemagglutination test for assay of antigen and antibody (a review). *Acta Microbiol. Hung.* **1991**, *38*, 81–90. [PubMed]
7. Gilmore, G.; Barnes, J.; Ketheesan, N.; Norton, R. Use of antigens derived from Burkholderia pseudomallei, *B. thailandensis*, and *B. cepacia* in the indirect hemagglutination assay for melioidosis. *Clin. Vaccine Immunol.* **2007**, *14*, 1529–1531. [CrossRef] [PubMed]
8. Tiyawisutsri, R.; Peacock, S.J.; Langa, S.; Limmathurotsakul, D.; Cheng, A.C.; Chierakul, W.; Chaowagul, W.; Day, N.P.J.; Wuthiekanun, V. Antibodies from patients with melioidosis recognize *Burkholderia mallei* but not *Burkholderia thailandensis* antigens in the indirect hemagglutination assay. *J. Clin. Microbiol.* **2005**, *43*, 4872–4874. [CrossRef] [PubMed]
9. Tandhavanant, S.; Wongsuvan, G.; Wuthiekanun, V.; Teerawattanasook, N.; Day, N.P.J.; Limmathurotsakul, D.; Peacock, S.J.; Chantratita, N. Monoclonal Antibody-Based Immunofluorescence Microscopy for the Rapid Identification of Burkholderia Pseudomallei in Clinical Specimens. *Am. J. Trop. Med. Hyg.* **2013**, *89*, 165–168. [CrossRef]
10. Posthuma-Trumpie, G.A.; Korf, J.; van Amerongen, A. Lateral flow (immuno) assay: Its strengths, weaknesses, opportunities and threats. A literature survey. *Anal. Bioanal. Chem.* **2009**, *393*, 569–582. [CrossRef]
11. Alrashoudi, A.A.; Albalawi, H.I.; Aldoukhi, A.H.; Moretti, M.; Bilalis, P.; Abedalthagafi, M.; Hauser, C.A.E. Fabrication of a Lateral Flow Assay for Rapid In-Field Detection of COVID-19 Antibodies using Additive Manufacturing Printing Technologies. *Int. J. Bioprint.* **2021**, *7*, 76–84. [CrossRef] [PubMed]
12. Hsiao, W.W.W.; Le, T.N.; Pham, D.M.; Ko, H.H.; Chang, H.C.; Lee, C.C.; Sharma, N.; Lee, C.K.; Chiang, W.H. Recent Advances in Novel Lateral Flow Technologies for Detection of COVID-19. *Biosensors* **2021**, *11*, 295. [CrossRef] [PubMed]
13. Nguyen, V.T.; Song, S.; Park, S.; Joo, C. Recent advances in high-sensitivity detection methods for paper-based lateral-flow assay. *Biosens. Bioelectron.* **2020**, *152*, 112015. [CrossRef] [PubMed]
14. Mao, X.; Wang, W.; Du, T.E. Dry-reagent nucleic acid biosensor based on blue dye doped latex beads and lateral flow strip. *Talanta* **2013**, *114*, 248–253. [CrossRef] [PubMed]
15. Sharma, A.; Tok, A.I.Y.; Lee, C.; Ganapathy, R.; Palaniappan, A.; Liedberg, B. Magnetic field assisted preconcentration of biomolecules for lateral flow assaying. *Sens. Actuators B Chem.* **2019**, *285*, 431–437. [CrossRef]
16. Hui, W.L.; Zhang, S.N.; Zhang, C.; Wan, Y.S.; Zhu, J.L.; Zhao, G.; Wu, S.D.; Xi, D.J.; Zhang, Q.L.; Li, N.N.; et al. A novel lateral flow assay based on GoldMag nanoparticles and its clinical applications for genotyping of MTHFR C677T polymorphisms. *Nanoscale* **2016**, *8*, 3579–3587. [CrossRef]

17. Zhang, X.Y.; Yu, X.Z.; Wen, K.; Li, C.L.; Marti, G.M.; Jiang, H.Y.; Shi, W.M.; Shen, J.Z.; Wang, Z.H. Multiplex Lateral Flow Immunoassays Based on Amorphous Carbon Nanoparticles for Detecting Three Fusarium Mycotoxins in Maize. *J. Agric. Food Chem.* **2017**, *65*, 8063–8071. [CrossRef]
18. Qin, K.M.; Ding, M.Y.; Zhang, C.S.; Zhang, X.J.; Mao, Y.X.; Dang, M.; Li, Z.Z.; Wang, Y.Y.; Zhang, S.H.; Sun, Y.H.; et al. Development of a sensitive monoclonal antibody-based immunochromatographic strip for neomycin detection in milk. *Food Agric. Immunol.* **2022**, *33*, 315–327. [CrossRef]
19. Chen, Y.; Fu, Q.Q.; Xie, J.; Wang, H.; Tang, Y. Development of a high sensitivity quantum dot-based fluorescent quenching lateral flow assay for the detection of zearalenone. *Anal. Bioanal. Chem.* **2019**, *411*, 2169–2175. [CrossRef]
20. Xu, L.D.; Wang, S.W.; Zhu, J.; Zhou, T.T.; Ding, S.N. Dendritic Silica Nanospheres Loaded with Red-Emissive Enhanced Carbon Dots for Zika Virus Immunoassay. *Chemistryselect* **2021**, *6*, 9787–9793. [CrossRef]
21. Xu, L.D.; Zhu, J.; Ding, S.N. Highly-fluorescent carbon dots grown onto dendritic silica nanospheres for anthrax protective antigen detection. *Anal. Methods* **2022**, *14*, 1836–1840. [CrossRef]
22. Hu, Q.S.; Wei, Q.Z.; Zhang, P.P.; Li, S.; Xue, L.; Yang, R.F.; Wang, C.B.; Zhou, L. An up-converting phosphor technology-based lateral flow assay for point-of-collection detection of morphine and methamphetamine in saliva. *Analyst* **2018**, *143*, 4646–4654. [CrossRef] [PubMed]
23. Seo, S.E.; Ryu, E.; Kim, J.; Shin, C.J.; Kwon, O.S. Fluorophore-encapsulated nanobeads for on-site, rapid, and sensitive lateral flow assay. *Sens. Actuators B Chem.* **2023**, *381*, 133364. [CrossRef] [PubMed]
24. Wen, C.Y.; Xie, H.Y.; Zhang, Z.L.; Wu, L.L.; Hu, J.; Tang, M.; Wu, M.; Pang, D.W. Fluorescent/magnetic micro/nano-spheres based on quantum dots and/or magnetic nanoparticles: Preparation, properties, and their applications in cancer studies. *Nanoscale* **2016**, *8*, 12406–12429. [CrossRef] [PubMed]
25. Raysyan, A.; Galvidis, I.A.; Schneider, R.J.; Eremin, S.A.; Burkin, M.A. Development of a latex particles-based lateral flow immunoassay for group determination of macrolide antibiotics in breast milk. *J. Pharm. Biomed. Anal.* **2020**, *189*, 113450. [CrossRef] [PubMed]
26. Chen, J.Y.; Luo, P.J.; Liu, Z.W.; He, Z.X.; Pang, Y.M.; Lei, H.T.; Xu, Z.L.; Wang, H.; Li, X.M. Rainbow latex microspheres lateral flow immunoassay with smartphone-based device for simultaneous detection of three mycotoxins in cereals. *Anal. Chim. Acta* **2022**, *1221*, 340138. [CrossRef]
27. Wang, Y.Y.; Xu, H.; Wei, M.; Gu, H.C.; Xu, Q.F.; Zhu, W. Study of superparamagnetic nanoparticles as labels in the quantitative lateral flow immunoassay. *Mater. Sci. Eng. C-Biomim. Supramol. Syst.* **2009**, *29*, 714–718. [CrossRef]
28. Xie, Z.H.; Feng, S.S.; Pei, F.B.; Xia, M.Z.; Hao, Q.L.; Liu, B.; Tong, Z.Y.; Wang, J.; Lei, W.; Mu, X.H. Magnetic/fluorescent dual-modal lateral flow immunoassay based on multifunctional nanobeads for rapid and accurate SARS-CoV-2 nucleocapsid protein detection. *Anal. Chim. Acta* **2022**, *1233*, 340486. [CrossRef]
29. Yan, L.Z.; Dou, L.N.; Bu, T.; Huang, Q.; Wang, R.; Yang, Q.F.; Huang, L.J.; Wang, J.L.; Zhang, D.H. Highly sensitive furazolidone monitoring in milk by a signal amplified lateral flow assay based on magnetite nanoparticles labeled dual-probe. *Food Chem.* **2018**, *261*, 131–138. [CrossRef]
30. He, H.; Liu, B.L.; Wen, S.H.; Liao, J.Y.; Lin, G.G.; Zhou, J.J.; Jin, D.Y. Quantitative Lateral Flow Strip Sensor using Highly Doped Upconversion Nanoparticles. *Anal. Chem.* **2018**, *90*, 12356–12360. [CrossRef]
31. Kim, H.S.; Ko, H.; Kang, M.J.; Pyun, J.C. Highly sensitive rapid test with chemiluminescent signal bands. *Biochip J.* **2010**, *4*, 155–160. [CrossRef]
32. Wang, Y.; Fill, C.; Nugen, S.R. Development of chemiluminescent lateral flow assay for the detection of nucleic acids. *Biosensors* **2012**, *2*, 32–42. [CrossRef] [PubMed]
33. Ren, Z.X.; Xu, L.Y.; Yang, L.; Cui, Y. Minimizing Cross-Reactivity for the Chemiluminescent Lateral Flow Immunoassay of Cardiac Troponin I Based on PEGylation of Gold Nanoparticles. *Anal. Chem.* **2023**, *95*, 6646–6654. [CrossRef]
34. Baker, S.N.; Baker, G.A. Luminescent Carbon Nanodots: Emergent Nanolights. *Angew. Chem. Int. Ed.* **2010**, *49*, 6726–6744. [CrossRef] [PubMed]
35. Xu, L.D.; Zhang, Q.; Ding, S.N.; Xu, J.J.; Chen, H.Y. Ultrasensitive Detection of Severe Fever with Thrombocytopenia Syndrome Virus Based on Immunofluorescent Carbon Dots/SiO_2 Nanosphere-Based Lateral Flow Assay. *Acs Omega* **2019**, *4*, 21431–21438. [CrossRef]
36. Shen, J.; Shang, S.M.; Chen, X.Y.; Wang, D.; Cai, Y. Facile synthesis of fluorescence carbon dots from sweet potato for Fe3+ sensing and cell imaging. *Mater. Sci. Eng. C Mater. Biol. Appl.* **2017**, *76*, 856–864. [CrossRef]
37. Shi, N.N.; Sun, K.Y.; Zhang, Z.D.; Zhao, J.; Geng, L.N.; Lei, Y.H. Amino-modified carbon dots as a functional platform for drug delivery: Load-release mechanism and cytotoxicity. *J. Ind. Eng. Chem.* **2021**, *101*, 372–378. [CrossRef]
38. Sun, Y.Q.; Li, J.A.; He, D.W.; Wang, X.R.; Shi, Y.; Pan, L.J. Recent progress on performances and mechanisms of carbon dots for gas sensing. *Luminescence* **2022**, *ahead of print*. [CrossRef]
39. Li, H.T.; He, X.D.; Kang, Z.H.; Huang, H.; Liu, Y.; Liu, J.L.; Lian, S.Y.; Tsang, C.H.A.; Yang, X.B.; Lee, S.T. Water-Soluble Fluorescent Carbon Quantum Dots and Photocatalyst Design. *Angew. Chem.-Int. Ed.* **2010**, *49*, 4430–4434. [CrossRef]
40. He, C.; Xu, P.; Zhang, X.H.; Long, W.J. The synthetic strategies, photoluminescence mechanisms and promising applications of carbon dots: Current state and future perspective. *Carbon* **2022**, *186*, 91–127. [CrossRef]

41. Houghton, R.L.; Reed, D.E.; Hubbard, M.A.; Dillon, M.J.; Chen, H.J.; Currie, B.J.; Mayo, M.; Sarovich, D.S.; Theobald, V.; Limmathurotsakul, D.; et al. Development of a Prototype Lateral Flow Immunoassay (LFI) for the Rapid Diagnosis of Melioidosis. *PLoS Negl. Trop. Dis.* **2014**, *8*, e2727. [CrossRef] [PubMed]
42. Aydin, S. A short history, principles, and types of ELISA, and our laboratory experience with peptide/protein analyses using ELISA. *Peptides* **2015**, *72*, 4–15. [CrossRef]
43. Zhou, T.T.; Yue, Y.; Zheng, F.; Liang, X.D.; Cao, Q.X.; Wang, Y.W.; Zhu, J. Monoclonal antibody against L-lectin module of SraP blocks adhesion and protects mice against Staphylococcus aureus challenge. *J. Microbiol. Immunol. Infect.* **2021**, *54*, 420–428. [CrossRef]
44. Radhakrishnan, A.; Behera, B.; Mishra, B.; Mohapatra, P.R.; Kumar, R.; Singh, A.K. Clinico-microbiological description and evaluation of rapid lateral flow immunoassay and PCR for detection of Burkholderia pseudomallei from patients hospitalized with sepsis and pneumonia: A twenty-one months study from Odisha, India. *Acta Trop.* **2021**, *221*, 105994. [CrossRef]
45. Shaw, T.; Tellapragada, C.; Vandana, K.E.; AuCoin, D.P.; Mukhopadhyayl, C. Performance evaluation of Active Melioidosis Detect-Lateral Flow Assay (AMD-LFA) for diagnosis of melioidosis in endemic settings with limited resources. *PLoS ONE* **2018**, *13*, e0194595. [CrossRef] [PubMed]
46. Wongsuvan, G.; Hantrakun, V.; Teparrukkul, P.; Imwong, M.; West, T.E.; Wuthiekanun, V.; Day, N.P.J.; AuCoin, D.; Limmathurotsakul, D. Sensitivity and specificity of a lateral flow immunoassay (LFI) in serum samples for diagnosis of melioidosis. *Trans. R. Soc. Trop. Med. Hyg.* **2018**, *112*, 568–570. [CrossRef] [PubMed]
47. Currie, B.J.; Woerle, C.; Mayo, M.; Meumann, E.M.; Baird, R.W. What is the Role of Lateral Flow Immunoassay for the Diagnosis of Melioidosis? *Open Forum Infect. Dis.* **2022**, *9*, ofac149. [CrossRef]